Published in final edited form as:
Dev Biol. 2013 January 1; 373(1): 118–129. doi:10.1016/j.ydbio.2012.10.011.

Role of the inositol polyphosphate-4-phosphatase type II Inpp4b in the generation of ovarian teratomas

Ashwini Balakrishnan and **J. Richard Chaillet**
Department of Microbiology and Molecular Genetics, Magee-Womens Research Institute, University of Pittsburgh, Pittsburgh, PA 15208 USA

Abstract

Teratomas are a unique class of tumors composed of ecto- meso- and endodermal tissues, all foreign to the site of origin. In humans, the most common teratoma is the ovarian teratoma. Not much is known about the molecular and genetic etiologies of these tumors. Female carriers of the *Tgkd* transgene are highly susceptible to developing teratomas. Ovaries of *Tgkd*/+ hemizygous female mice exhibit defects in luteinization, with numerous corpora lutea, some of which contain central trapped, fully-grown oocytes. Genetically, *Tgkd* teratomas originate from mature oocytes that have completed meiosis I, suggesting that *Tgkd* teratomas originate from these trapped oocytes. The insertion of *Tgkd* 3′ of the *Inpp4b* gene is associated with decreased expression of *Inpp4b* and changes in intracellular PI3 Kinase/AKT signaling in follicular granulosa cells. Because *Inpp4b* is not expressed in fully-grown wild-type or *Tgkd* oocytes, these findings suggest that hyperactivation of the PI3K/AKT pathway caused by the decrease in INPP4B in granulosa cells promotes an ovarian environment defective in folliculogenesis and conducive to teratoma formation.

Keywords

teratoma; PI3-kinase/AKT; Inpp4b; oocyte; granulosa

INTRODUCTION

Ovarian teratomas (OTs) are tumors of the ovary derived from non-ovulated female germ cells that have undergone parthenogenetic activation and display a disorganized pattern of cellular differentiation (Linder et al., 1975; Ulbright 2005). Human OTs are relatively common, constituting 95% of all ovarian germ cell tumors (Ulbright 2005). Most OTs are benign but a small percentage (1–2%) transform into malignant tumors (Schmid-Braz et al., 2002). OTs contributed to 1.5% of the invasive ovarian cancer cases in the United States between 2004 and 2008 (Howlader et al., 2011). OTs are also seen at a low frequency in other mammalian species, including the mouse (Stevens and Varnum 1974). Most OTs are benign and are composed of differentiated ectodermal, mesodermal and endodermal tissues, proportions varying from teratoma to teratoma. Immature OTs contain undifferentiated cells (primarily immature neuroepithelium or embryonal carcinoma cells) in addition to the differentiated tissues and have malignant potential.

Corresponding author: J. Richard Chaillet, chailletjr@mwri.magee.edu, phone: (412) 641-8166.

Human OTs originate from oocytes at all meiotic stages, although most develop from oocytes that have completed meiosis I (Carritt et al., 1982; Deka et al., 1990; Muretto et al., 2001; Parrington et al., 1984; Surti et al., 1990; Hoffner et al., 1992). Rarely, benign cystic ovarian teratoma and specific malignant germ cell tumor cases have been observed within families, suggesting one or more underlying genetic etiologies (Blake et al., 1993; Brenner et al., 1983; Indinnimeo et al., 2003; Plattner et al., 1973; Simon et al., 1985; Stettner et al., 1999). However, the majority of OTs occur sporadically. No associations with known genetic loci have been established in either familial or sporadic OT cases. The absence of a clear genetic association raises the possibilities that mutations in many different genes can cause OTs or that non-genetic etiologies are common.

Mouse strains predisposed to developing OTs have provided insight into their development. LT/Sv is an inbred mouse strain in which approximately 50% of the females develop OTs by 90 days of age (Stevens and Varnum 1974). These OTs originated from parthenogenetically activated oocytes that have completed meiosis 1 (Eppig et al., 1977). LT/Sv oocytes experience a prolonged period of meiotic arrest at metaphase I (MI) (O'Neill and Kaufman 1987). This arrest (delayed metaphase to anaphase I transition) has been linked to the sustained activity of maturation promoting factor (MPF), a complex of CDK1 and cyclin B (Hampl and Eppig 1995). Normally, a decrease in MPF activity is required for resumption of meiosis I, and sustained MPF activity and MI arrest may predispose unfertilized LT/Sv oocytes to spontaneous cell division (parthenogenesis) and OT formation. Prolonged metaphase I arrest and parthenogenetic activation of oocytes have been reported to be necessary but not sufficient for OT formation (Eppig et al., 1996). Other requirements for OT formation have been revealed in an analysis of crosses between C57BL/6 and LT/Sv mice, which identified OT susceptibility loci, including a prominent locus (*Ots1*) on chromosome 6 (Lee et al., 1997).

Targeted mutagenesis in mice has also produced mouse strains susceptible to developing OTs. The *c-mos* gene encodes the cytostatic factor responsible for metaphase II arrest. Consequently, oocytes of homozygous *c-mos*-null mice fail to maintain metaphase II arrest and spontaneously initiate parthenogenetic embryonic development in the absence of fertilization. Approximately 40% of *c-mos*-null mice develop OTs (Colledge et al., 1994; Hashimoto et al., 1994). Mutations in the coding region of the human *c-MOS* gene have not been reported, suggesting that mutations in the *c-MOS* gene do not play a role in the genesis of human OTs (de Foy et al., 1998). The *MommeR1* mouse strain with a missense mutation in the transcription factor *Foxo3a* is predisposed to developing OTs; one-sixth of homozygous *MommeRI* females develop OTs (Youngson et al., 2011). The missense mutation was found to cause a decrease in the transactivation potential of the transcription factor FOXO3A. Notably, both FOXO3A and c-MOS proteins are primarily expressed in the oocyte, with little expression in somatic cells of the ovary (Goldman et al., 1987; John et al., 2008).

Genetic defects in genes expressed in follicular granulosa cells (GCs), but not in oocytes, also lead to OT formation in mice. One fifth of mFshr^{D580H} transgenic mice expressing a constitutively active form of the follicle-stimulating hormone (FSH) receptor in GCs develop OTs (Peltoketo et al., 2010). Similarly, overexpression of the *Bcl-2* gene in mouse GCs led to a 20% incidence of OTs (Hsu et al., 1996). Hence alteration in normal cell signaling within the GCs can predispose to OTs. Transgenic mice expressing small interfering RNAs (siRNAs) targeting the *Gata4* (si*Gata4*) gene also developed OTs (Thurisch et al., 2009). In the mouse ovary GATA4 is primarily expressed in GCs (Heikinheimo et al., 1997). Although the mechanism of OT formation in this model is presently unknown, it is possible that a decrease in granulosa-cell GATA4 indirectly influences oocyte function, leading to OT formation. Taken together, the molecular and

functional abnormalities observed in the various OT mouse models suggest that several distinct cell-signaling or cell-cycle defects in cells of the ovarian follicle can mediate OT development.

We have previously reported that 15–20% of hemizygous female carriers of the imprinted *Tgkd* transgene develop OTs in the inbred FVB/N (FVB) strain (Fafalios et al., 1996). OTs in the FVB-*Tgkd* strain have a malignant mixed germ cell phenotype (teratocarcinoma) with evidence of metastases to the mesenteric lymph node and lung. Because numerous other transgenic mouse lines with the same or related imprinted trangenes did not develop ovarian teratomas, we postulated that the development of OTs in FVB-*Tgkd* females is due to disruptions in one or more genes near the genomic site of transgene integration on mouse chromosome 8. We also observed that hemizygous *Tgkd* mice developed OTs only on the FVB strain and linkage analysis mapped the FVB-specific modifier locus to chromosome 6 (Eicher et al., manuscript in preparation). In this study, we examined the genetic and molecular effects of the *Tgkd* transgene on OT formation in FVB-*Tgkd* (henceforth designated *Tgkd*) mice.

RESULTS

Abnormal ovarian follicle development in Tgkd mice

We first examined ovaries of *Tgkd* mice for defects in folliculogenesis, previously reported in other OT susceptible strains (Peltoketo et al., 2010, Youngson et al., 2011). Follicles were typed using the Pedersen and Peters method of follicle classification (Pedersen and Peters 1968). The distribution of follicle types differed in prepubertal (23 days after birth or PD23) wildtype (FVB) and *Tgkd* mice, although the total number of activated follicles was not significantly different. Absolute numbers of primary (Type 3b – 1 layer of cuboidal GCs) and secondary (Type 4 – 2 layers of GCs) follicles were similar in wildtype and *Tgkd* ovaries, but there were twice the number of preantral (Type 5 – 3 or more layers of GCs) follicles in *Tgkd* ovaries (Figure 1A). This was accompanied by a decrease in the absolute number of early and late antral (Type 6–8) follicles per ovary. Similar defects in folliculogenesis were seen in post-pubertal PD30 *Tgkd* female mice. Specifically, we observed a 1.6-fold increase in the number of preantral follicles in PD30 *Tgkd* mice, which was accompanied by a 0.4-fold decrease in the number of antral follicles (Figure 1A).

PD30 *Tgkd* ovaries showed additional follicular defects, not present in age-matched wildtype mice, which are indicative of perturbed follicle maturation. An average of 4.4 corpora lutea were observed, whereas no corpora lutea were observed in control wildtype mice (Figure 1B). In addition, trapped oocytes were observed in many PD30 *Tgkd* corpora lutea (Figure 1C); one examined ovary contained four corpora lutea with trapped oocytes. A corpus luteum is formed from the remnants of the follicle after ovulation of the oocyte; hence a trapped oocyte indicates that the follicle has luteinized prior to ovulation of the oocyte. These luteinized, unruptured follicles are a further indication of defective ovarian follicle maturation in *Tgkd* mice, and the associated OTs may form via parthenogenetic activation of these oocytes. Despite the observed abnormalities in *Tgkd* ovary morphology, there was no evidence of a significant reduction in the fertility of hemizygous *Tgkd* females, and no differences in primordial follicle numbers between wildtype and *Tgkd* mice at both PD23 and PD30 (Supplementary Figure 1A and 1B). Consequently there was no evidence of premature ovarian failure (POF), which is associated with OT formation in other mouse strains (Peltoketo et al., 2010, Youngson et al., 2011). In addition, female *Tgkd* mice attained puberty at post-natal day 28 (PD28), the same day on which control wildtype female mice reached puberty (data not shown). This latter observation is consistent with normal gonadotrophin signaling during puberty in *Tgkd* female mice.

Tgkd oocytes complete meiosis I prior to forming OTs

Both follicle luteinization and meiotic maturation of fully-grown oocytes require luteinizing hormone (LH) (Hsieh et al., 2007). Therefore, if *Tgkd* OTs originate from oocytes trapped in corpora lutea we might expect them to have completed meiosis I. Using a single *Tgkd* transgene flanking DNA fragment (~38 cM from centromere) for genotyping, we previously reported hemizygous *Tgkd* genotypes in 5 OTs from hemizygous FVB-*Tgkd* female mice, suggesting a pre-meiotic origin of *Tgkd* OTs (Fafalios et al., 1996). However, this was an inconclusive study because of the use of a single heteromorphic marker located ~38 cM from the centromere of chromosome 8 (Fafalios et al., 1996). To more definitively determine the cellular etiology of *Tgkd* OTs, we studied genomic DNA samples from *Tgkd* OTs and paired host spleens obtained from *Tgkd* transgenic offspring of F1 (FVB-*Tgkd* x C57BL/6) hybrid male mice backcrossed to inbred FVB female mice (Eicher et al., manuscript in preparation). Genotypes of paired OT and spleen DNA samples were compared using pericentric and distal single nucleotide polymorphisms (SNPs) between FVB and C57BL/6 (B6) strains for each autosome and the X chromosome. For the majority of informative (heterozygous FVB/B6) pericentric markers in each spleen DNA sample, genotypes of the paired OT DNA sample were homozygous (Figure 2A, Supplementary Table 1). In contrast, the majority of the informative distal SNPs in each spleen DNA sample remained heterozygous in the OT, consistent with frequent meiotic recombination between a distal SNP marker and the centromere of the same chromosome. The small number of pericentric SNPs that were heterozygous in both paired OT and spleen DNA was likely due to a low frequency of recombination events near the centromere. We conclude from these findings that each of the seven examined *Tgkd* OTs originated from a single mature oocyte that had completed meiosis I.

Parthenogenetic activation of Tgkd oocytes

Parthenogenetic activation of oocytes has been reported to play a prominent role in the development of OTs (College et al., 1994, Hashimoto et al., 1994, Stevens and Varnum 1975). Given this, we measured spontaneous parthenogenetic activation in cultured unfertilized *Tgkd* oocytes by measuring the frequency of oocytes that progressed to the 2-cell stage (Eppig et al., 1996). Approximately 30% of cultured *Tgkd* oocytes underwent cell division, similar to the percentage of 2-cell embryos seen in cultured wildtype oocytes (Figure 2B). This rate of parthenogenetic activation of FVB oocytes is much greater than that of B6 oocytes (Eppig et al., 1996), suggesting that mature oocytes in inbred FVB mice have a propensity toward parthenogenetic activation. The absence of OTs in inbred FVB female mice however indicates that the FVB strain background alone is not sufficient for OT formation.

Role of oocyte Tgkd methylation in formation of OTs

Because the *Tgkd* transgene is maternally imprinted in *Tgkd* mice (Chaillet et al., 1995), we determined whether loss of *Tgkd* transgene methylation influenced the formation of *Tgkd* OTs. The Rous sarcoma virus (RSV) sequences of *Tgkd* are methylated on the maternal and unmethylated on the paternal *Tgkd* alleles (Chaillet et al., 1995). RSV sequences were highly methylated in *Tgkd Dnmt3l*$^{+/+}$ metaphase II arrested (MII) oocytes (82%) and *Tgkd* OTs (84%), but poorly methylated in *Tgkd Dnmt3l* $_{-/-}$ MII oocytes (26%) (Figure 3A). These findings are consistent with the known role of the DNMT3L protein in the establishment of genomic methylation, including imprinted methylation, during development of mouse MII oocytes (Bourc'his et al., 2001). OTs were found in *Tgkd* and *Tgkd Dnmt3l*$^{+/-}$ heterozygous female mice, but not in *Tgkd, Dnmt3l*$^{-/-}$ female mice (Figure 3B). These findings support the notion that oocyte genomic methylation, and possibly specifically *Tgkd* transgene methylation, is required for OT formation in *Tgkd* female mice.

Integration site of Tgkd transgene

To explore the molecular basis of *Tgkd* OTs, we identified the genomic location into which the *Tgkd* transgene inserted. Sequences of the endogenous genomic ends of both junctional fragments containing endogenous and *Tgkd* transgene sequences aligned with sequences on mouse chromosome 8, between the *Inpp4b* and *I15* genes. Further analysis of the junctional fragments indicated that approximately one kilobase of endogenous genomic DNA was deleted from the insertion site. The *Tgkd* transgene is located ~65 kilobases 3′ of the known 3′ end of the inositol polyphosphate-4-phosphatase type II (*Inpp4b*) gene and ~120 kilobases 5′ of the known 5′ end of the Interleukin 15 (*Il5*) gene (Figure 4A). The location of the large *Tgkd* transgene array in the intergenic region of *Inpp4b* and *Il15* suggested that the phenotypic abnormalities in *Tgkd* mice were due to disruption of one or more unidentified genes in the intergenic region or due to effects on *Inpp4b* and/or *Il15* gene function. No spliced or unspliced transcripts have been reported in the *Inpp4b-Il15* intergenic region and multiple attempts to recover exons in this intergenic region using exon-trapping strategies failed.

The Tgkd allele is associated with a decrease in Inpp4b expression

Il15 is not likely to play a role in the etiology of OTs because *Il15* is mainly involved in the innate immune response (Ohteki et al., 2001), and neither $Il15^{-/-}$ mice nor mice that overexpress IL15 have been reported to develop OTs (Kennedy et al., 2000, Fehniger et al., 2001). We therefore postulate that the phenotypic abnormalities in *Tgkd* mice are due to abnormalities in expression of the *Inpp4b* gene. Because *Inpp4b* transcripts are highly expressed in the brain, we first explored the effect of the *Tgkd* insertion on *Inpp4b* transcript and protein levels in the heads of embryonic day 13.5 (E13.5) embryos (Ferron and Vacher 2006). The two main *Inpp4b* transcripts, *Inpp4bα* and *Inpp4bβ* are produced by alternative splicing of the 3′ end of *Inpp4b* and are translated into the INPP4Bα and INPP4Bβ proteins respectively (Ferron and Vacher 2006). A comparison of *Inpp4b* transcript levels was performed among *Tgkd/Tgkd*, *Tgkd*(mat)*/+* (maternal inheritance), *Tgkd*(pat)*/+* (paternal inheritance) and wild-type E13.5 embryos (Figure 5A). The level of *Inpp4bβ* was most affected by the *Tgkd* insertion; *Tgkd/Tgkd* and *Tgkd*(mat)/+ embryos expressed ~50% of wild-type *Inpp4bβ*, whereas *Tgkd*(pat)/+ embryos showed an ~20% decease in *Inpp4bβ* expression. *Inpp4bα* (includes *Inpp4bα.s,* a short α-like transcript) was less affected in *Tgkd* embryo heads. Homozygous *Tgkd/Tgkd* embryos showed the most downregulation (20%) compared to wildtype controls, and *Tgkd*(mat)/+ embryos had comparable *Inpp4bα* expression as *Tgkd/Tgkd* embryos. Levels of *Inpp4bα* in *Tgkd*(pat)/+ embryos were somewhat lower than wildtype embryos but this difference was not statistically significant. Total *Inpp4b* followed a pattern of expression similar to the *Inpp4bα* transcript because the level of *Inpp4bβ* was approximately 10-fold lower than the total levels of *Inpp4b* in adult brain. INPP4B protein levels were correspondingly reduced in E13.5 embryonic heads. Individual *Tgkd/Tgkd* heads had ~50% of the wildtype protein concentration (Figure 5B). Individual *Tgkd*(mat) and *Tgkd*(pat) heads had lower concentrations of INPP4B, although collectively, levels of INPP4B in hemizygous mice were not statistically different than wild-type mice (Figure 5B). The combination of small effects on the normally highly expressed *Inpp4bα* transcripts, and large effects on the normally poorly expressed *Inpp4bβ* transcript from both parental *Tgkd* alleles accounts for the significant differences in INPP4B expression between *Tgkd*/*Tgkd* and control wildtype embryos. Because there was no significant effect of *Tgkd* parental origin on INPP4B protein expression, we did not distinguish *Tgkd*(mat) from *Tgkd*(pat) female mice in studies of effects of the *Tgkd* transgene in the ovary.

RNA *in situ* hybridization (ISH) was used to determine the location of *Inpp4b* transcripts. As shown in Figure 6A, the *Inpp4bα*, but not the *Inpp4bβ* isoform was expressed in the

ovary and this expression was confined to GCs. No expression was observed in oocytes. These findings were confirmed in measurements of individual *Inpp4b* transcripts in isolated GCs and oocytes in PD30 wildtype and *Tgkd* mice (Figure 6B). The surprising finding that ovarian *Inpp4b* expression is confined to GCs raises the possibility that the *Tgkd* insertion facilitates OT formation by altering INPP4B expression in GCs, which in turn alters follicular development and possibly normal GC-oocyte interactions. In addition, *Inpp4b* expression is known to be responsive to androgens (Hodgson et al., 2011). For these reasons, we examined the effect of *Tgkd* on INPP4B levels in ovarian cells exposed to hormonal stimuli. No difference in expression of *Inpp4b* was observed between PD23 wildtype and *Tgkd* ovaries (Figure 6C). Synchronized *in vivo* maturation of wildtype and *Tgkd* ovarian follicles was initiated with gonadotrophins (one-time IP injection of pregnant mare serum gonadotrophin (PMSG)), followed by induction of ovulation with a one-time injection of human chorionic gonadotropin (HCG). Levels of *Inpp4b* in wildtype mice fluctuated over the 48-hour time course of PMSG stimulation and 2 hours of HCG stimulation. The *Tgkd* mice show a 20% decrease in the level of *Inpp4b* transcript compared to the wildtype mice at 24 and 38 hours after PMSG stimulation (Figure 6C). A slightly larger difference was seen between wildtype and *Tgkd* ovaries 48 hours after PMSG stimulation, where *Tgkd* ovaries expressed 70% of wildtype levels of *Inpp4b*.

The *Tgkd* transgene also affected levels of ovarian INPP4B protein. INPP4B levels in lysates of whole ovaries fluctuated slightly during the time course of PMSG stimulation. The largest difference, a 50% decrease of INPP4B in *Tgkd* ovaries ($p<0.05$), was recorded 38 hours after PMSG stimulation (Figure 6D). At other time points during PMSG stimulation, the levels of INPP4B were comparable in wildtype and *Tgkd* mice. A more pronounced effect of the transgene on INPP4B expression was observed in purified and *in-vitro* cultured GCs; INPP4B was significantly downregulated to a higher extent in cultured unstimulated PD23 *Tgkd* GCs (70% of wildtype GCs) and following 10 minutes of FSH administration (Figure 6E). This method of enriching for GCs excluded the ovarian capsule and stroma, which expressed low levels of *Inpp4b* (Supplementary Figure 1D&E).

Tgkd affects PI3K/AKT signaling in ovarian follicles

Because *Inpp4b* has been implicated in the control of intracellular PI3-Kinase/AKT (PI3K/AKT) signaling (Figure 7A; Gewinner et al., 2009; Fedele et al., 2010; Hodgson et al., 2011), we studied the effects of the *Tgkd* transgene on PI3K/AKT signaling in the ovary. Whole ovaries were collected at different time points following *in-vivo* hormonal stimulation, and the time course of phosphorylated AKT (P-AKT), an indication of PI3K/AKT pathway activation, and its downstream effects were measured. P-AKT levels were roughly similar in immature PD23 wildtype and *Tgkd* ovaries prior to administration of exogenous hormones, but significant differences were evident following 14 and 24 hours of PMSG stimulation ($p<0.05$) (Figure 7B; Quantified in Supplementary Figure 3A). Corresponding differences in levels of phosphorylated FOXO1 (P-FOXO1), a downstream target of P-AKT (Figure 7A) specifically in GCs, was also evident (Figure 7B) (Richards et al., 2002). Time courses of changes in total FOXO1, E2F1, CyclinD2 and P27 were similar between wildtype and *Tgkd* ovaries (Figure 7B). Following administration of a single dose of HCG 48 hours after PMSG stimulation, P-AKT and P-FOXO1 concentrations declined at a much faster rate in *Tgkd* compared to wildtype ovaries (Figure 7C; Quantified in Supplementary Figure 3B). An accentuated rate of decline in the level of FOXO1 and an accentuated rate of increase in CyclinD2 levels in *Tgkd* ovaries at specific time points following HCG stimulation were also evident (Figure 7C). We conclude from this experiment that the presence of the *Tgkd* transgene 3′ of the *Inpp4b* gene augments the response of mature ovarian follicles to stimuli known to mimic endogenous ovulatory

stimuli, leading to premature phosphorylation of the AKT protein and activation of downstream effectors of the PI3K/AKT signaling pathway.

The pattern of P-AKT activation following gonadotropin administration was investigated in wildtype and *Tgkd* oocytes. There was no difference in the P-AKT activation and phosphorylation of its downstream target FOXO3A between wildtype and *Tgkd* oocytes during the time course of gonadotrophin stimulation (Figure 7D). These findings are consistent with the observed absence of *Inpp4b* expression in fully-grown oocytes (Figure 6).

Collectively, the observed effects of the *Tgkd* transgene on ovarian and oocyte AKT signaling are consistent with effects of *Tgkd* on PI3K/AKT signaling in GCs. To directly test this postulate, we obtained purified GC pools and stimulated them with FSH. *Tgkd* GCs from PD23 ovaries had a lower level of INPP4B than wildtype GCs (Figure 6E). *Tgkd* GCs also had a slightly higher level of P-AKT and P-FOXO1 after overnight culture in medium containing 10% FBS (Figure 7E; Quantified in Supplementary Figure 4). *Tgkd* GCs did not show the decline in P-AKT levels seen in wildtype GCs after 40 minutes of FSH stimulation (Figure 7E; Quantified in Supplementary Figure 4). We independently investigated this inverse relationship between INPP4B levels and AKT pathway activation in GCs infected with lentiviruses expressing shRNAs to the mouse *Inpp4b* gene. Two independent shRNA constructs were used, and expression of both constructs resulted in 50% reduction in the levels of INPP4B compared to controlled uninfected wildtype GCs (Figure 7F). Corresponding increases in the levels of P-AKT and P-FOXO1 were seen prior to and 40 minutes after FSH administration. These results confirm the relationship between INPP4B and PI3K/AKT signaling observed in *Tgkd* GCs. Notably, not all *Tgkd* cells show a decrease in the level of INPP4B and augmented effects on PI3K/AKT signaling following stimulation. For example, hemizygous and homozygous *Tgkd* ES cell lines derived from *Tgkd* embryos did not show a consistent decrease in steady-state INPP4B levels and effects of *Tgkd* on the PI3K/AKT signaling pathway were not evident upon standard stimulation with IGF1 (Supplementary Figure 2).

Proliferation and apoptosis of GCs were altered in Tgkd ovaries

Downstream effectors of AKT activation have been shown to induce cell proliferation and block apoptosis (Manning and Cantley 2007). Cyclin D2 promotes G1/S phase transition and increase cell proliferation, and FOXO1 is known to promote cellular apoptosis (Sherr CJ. 1995, Huang and Tindall 2007). Because the levels of P-AKT and downstream targets FOXO1 and Cyclin D2 in the ovary are influenced by *Tgkd* (Figure 7C), we compared rates of cell proliferation and apoptosis in preantral and antral follicles of *Tgkd* and wildtype female mice (Fan et al., 2008a and b). There was a significant 1.8-fold increase in the rate of GC proliferation in PD30 *Tgkd* ovaries (Figure 8A). The rate of apoptosis in *Tgkd* ovaries was also significantly reduced to approximately 50% of the rate seen in wildtype ovaries as measured by cleaved caspase 3 staining at 2 hours after HCG stimulation (Figure 8B). FOXO1 localization was similar in follicles of wildtype and *Tgkd* PD30 ovaries (Supplementary Figure 5). These results further reinforce the notion that follicle maturation is perturbed in *Tgkd* ovaries through the premature phosphorylation of AKT and FOXO1 in GCs, and imbalances in rates of cellular proliferation and apoptosis.

DISCUSSION

Altered kinetics of the PI3K/AKT pathway leads to OT development

Inpp4b is a recently identified suppressor of the PI3K/AKT signal transduction pathway that has not been studied previously in the ovary (Gewinner et al., 2009, Fedele et al., 2010,

Hodgson et al., 2011). *Inpp4b* is an inositol-polyphosphate-4-phosphatase, whose main substrate is phosphatidylinositol 3,4 bisphosphate ($PI(3,4)P_2$), which it dephosphorylates to phosphatidylinositol-3-phosphate PI(3)P. Because $PI(3,4)P_2$ stimulates AKT phosphorylation, a decrease in *Inpp4b* levels has been linked to increased AKT activation and the progression of breast, ovarian and prostrate cancer (Gewinner et al., 2009, Fedele et al., 2010, Hodgson et al., 2011). In this study, we established a link between PI3K/AKT signaling and OT development in *Tgkd* mice by showing that low levels of this novel inositol phosphatase in follicular granulosa cells (GCs) wwleads to the development of OTs. Specifically, a decrease in *Inpp4b* levels in GCs during gonadotrophin stimulation is associated with hyperactivation of the PI3K/AKT pathway, which is reflected by an increase in AKT phosphorylation and subsequent FOXO1 phosphorylation in *Tgkd* GCs. The hyperactivation of the PI3K/AKT pathway is accompanied by an increase in proliferation and decrease in apoptosis in *Tgkd* GCs. These changes lead to multiple defects in folliculogenesis including an increase in preantral follicles and premature appearance of corpora lutea in *Tgkd* mice. Moreover, a subset of lutenized follicles in *Tgkd* ovaries contain mature oocytes trapped within them, and the oocytes of the FVB strain have a high parthenogenetic activation rate, independent of the *Tgkd* transgene. We speculate that the combination of luteinized unruptured follicles observed in the *Tgkd* strain resulting from *Inpp4b* reduction in GCs and the high innate parthenogenetic activation rate of FVB oocytes predispose *Tgkd* mice to OTs.

PI3K/AKT is an essential signal transduction pathway in the ovary, involved in follicle recruitment and induction of many important FSH-mediated follicular maturation events including GC proliferation, differentiation, cumulus cell expansion, and meiotic resumption of oocytes (Zeleznik et al., 2003; Shimada et al., 2003; Hoshino et al., 2004; Kalous et al., 2006; Han et al., 2006). Studies of mouse PTEN, a better characterized suppressor of the PI3K/AKT pathway than INPP4B, nicely illustrate the diverse cellular roles of this important intracellular signaling pathway. Ablation of the *Pten* gene in oocytes leads to premature follicle recruitment and ovarian failure leading to infertility in early adulthood, while deletion of both *Pten* alleles in GCs results in enhanced GC proliferation, decreased GC apoptosis, persistence of multiple corpora lutea and unexpected increases in litter size (Reddy et al., 2008; Fan et al., 2008a). *Pten* and *Inpp4b* suppress the PI3K/AKT pathway by degrading $PI(3,4,5)P_3$ and $PI(3,4)P_2$ respectively, the chief activators of AKT (Figure 7; Maehama and Dixon 1998; Norris et al., 1997; Gewinner et al., 2009). *Tgkd* GCs with decreased *Inpp4b* levels show a similar increase in proliferation and decrease in apoptosis to that observed in GCs depleted of PTEN, but the rate of corpora lutea clearance in *Tgkd* ovaries was unaffected by the decrease in *Inpp4b* levels (Supplementary Figure 1C).

Molecular events both upstream and downstream of follicular AKT activation have been previously implicated in OT development. Forced expression of a constitutively active form of the FSH receptor (FSHR) from a transgene ($mFshr^{D580H}$) in GCs causes OTs in 20% of transgene carriers and FSHR signaling is associated with activation of the PI3K/AKT pathway (Peltoketo et al., 2010;Gonzalez-Robayna et al., 2000). Furthermore, a reduction in FOXO3A activity, a downstream effect of increased AKT activation is associated with OT development (Youngson et al., 2011). FOXO3A is primarily expressed in oocytes, not GCs and is phosphorylated by activated AKT, causing its nuclear exclusion, degradation and loss of its transcriptional activation (John et al. 2008; Huang and Tindall 2007). Interestingly, a missense mutation in the mouse *Foxo3a* gene in the *MommeR1* mouse strain directly decreases its transcriptional activation, mimicking the effect of increased oocyte PI3K/AKT pathway activity on FOXO3A, which causes one out of every six homozygous mutant *MommeR1* female mice to develop OTs (Youngson et al., 2011). In summary, the $mFshr^{D580H}$ and *Tgkd* transgenes illustrate the relationship between hyperactivation of the

GC PI3K/AKT pathway and OT formation, while the *MommeR1* strain illustrates the same relationship, but in oocytes.

Effect of Inpp4b levels on OT phenotype

Ovarian phenotypes appear to be exquisitely sensitive to the cell type and/or extent of gene disruption. For example, while a decrease in *Foxo3a* activity in *MommeR1* mice causes OTs, complete loss of oocyte FOXO3A activity is associated with POF, without the occurrence of OTs (Castrillon et al., 2003). Similarly, the level of ovarian transgene expression of $mFshr^{D580H}$ correlates with the severity of the ovarian phenotype (Peltoketo et al., 2010). Our studies indicate that a small decrease in GC *Inpp4b* in *Tgkd* mice is sufficient to alter AKT activation kinetics in GCs, leading to a variety of abnormal ovarian phenotypes including OTs. We can speculate that lesser or greater degrees of INPP4B defects would produce a different and unique collection of abnormal ovarian phenotypes, including ones that might preclude OT formation.

Recently an *Inpp4b* knockout mouse has been generated through the *Cre* mediated deletion of exon 11(Ferron et al., 2011). Adult $Inpp4b^{-/-}$ mice are reported to be viable and do not develop OTs or spontaneous cancers, even though *Inpp4b* reduction has been previously linked to the etiology of breast and prostrate cancer (Gewinner et al., 2009, Fedele et al., 2010, Hodgson et al., 2011). Sustained loss of INPP4B in $Inpp4b^{-/-}$ mice may have led to adaptation by other suppressors of the PI3K/AKT pathway. Further, the mechanism by which the *Tgkd* transgene causes a decrease in *Inpp4b* levels is currently unknown. The insertion could have disrupted an enhancer or changed local chromatin configuration, which leads to sudden or cell-specific changes, preventing adaptation by other components of the pathway. The insertion could have affected other genes on chromosome 8, but a preliminary screen did not detect any other transcriptional differences in genes in a 2MB region surrounding the *Tgkd* transgene. We also have not identified any sequence changes in the body of the *Tgkd*-linked *Inpp4b* gene nor novel forms of *Inpp4b* mRNAs in homozygous *Tgkd* E13.5 brains.

OT development is a multifactorial process

OT formation has been linked to signaling defects in either oocytes or in the surrounding follicular GCs. Other OT mouse models, particularly those with defects in GCs, share aspects of *Tgkd* ovarian pathology. The intentional genetic defects in the $mFshr^{D580H}$, *Inhα-bcl2* and si*Gata4* mouse lines are all confined to GCs (Peltoketo et al., 2010; Hsu et al., 1996; Thurisch et al., 2009). Interestingly the $mFshr^{D580H}$ model shows an increase in GC proliferation, while *Inhα-bcl2* ovaries display a decrease in GC apoptosis. Luteinized follicles containing trapped oocytes are seen in $mFshr^{D580H}$ mice (Peltoketo et al., 2010). All of these processes are affected in female *Tgkd* mice, which have a high incidence of OTs, suggesting that the collective influence of many altered follicular processes greatly enhances the likelihood of OT formation.

We also observed that *Tgkd Dnmt3l* $_{-/-}$ mice did not develop OTs. Methylation of the *Tgkd* transgene and all endogenous maternal methylation imprints should not be established in *Tgkd Dnmt3l* $_{-/-}$ oocytes (Bourc'his et al., 2001). Because *Inpp4b* is expressed in GCs, but not in oocytes, the parental origin of *Tgkd*, and hence the extent of its methylation, may not play a role in OT formation because mice with GCs inheriting *Tgkd* from either parent develop OTs (Fafalios et al., 1996). Rather, the requirement of maternal methylation imprints for OT formation may be due to the strict requirement of maternal imprints for embryogenesis (Bourc'his et al., 2001), a process mimicked in the growth and cellular differentiation of OTs.

Because a common feature of many mouse strains developing OTs is the FVB strain background, we must consider the possibility that these influences on OT development are determined by FVB alleles of other genes. The *Tgkd*, *mFshr*^{D580H}, *Inhα-bcl2* and *MommeR1* strains have been reported to develop OTs on the FVB background (Fafalios et al., 1996; Peltoketo et al., 2010; Hsu et al., 1996; Youngson et al., 2011), and FVB oocytes possess a high parthenogenetic activation rate, which is required for OT formation (Eppig et al., 1996). In this regard, an FVB-specific OT modifier locus has been mapped to chromosome 6, within a region that overlaps a previously mapped LT/Sv strain-specific OT modifier effect (Eicher et al., manuscript in preparation; Lee et al., 1997). Identification of candidate genes within this region that contribute to the OT phenotype would help better understand the multifactorial processes involved in the generation of teratomas. The effect of the FVB strain background may also explain the lack of the OT phenotype in the *Inpp4b*$^{-/-}$ mice, which were studied in the C57BL/6 strain background.

In summary, altered regulation of the PI3K/AKT pathway caused by a decrease in *Inpp4b* in GCs during follicle maturation leads to a dramatic increase in the number of GCs. This is associated with several follicular defects including oocytes trapped within luteinized follicles. The trapped oocytes caused by the *Tgkd* transgene combined with the parthenogenetic oocytes of the FVB strain predispose *Tgkd* mice to OT development.

MATERIAL AND METHODS

Animals

The *Tgkd* transgene was maintained on the inbred FVB/N (FVB) background as described previously (Fafalios et al., 1996). All experiments were performed in compliance with guidelines established by the Institutional Animal Care and Use Committee of the University of Pittsburgh. For determining the onset of puberty, females were examined daily for vaginal opening from day 22 postpartum.

SNP genotyping of ovarian teratomas (OT)

Spleen and teratoma DNA samples were collected from female progeny of the backcross of F1 (FVB-*Tgkd* X C57BL/6) to FVB/N mice. 20 pericentric and 20 distal SNPs (one per chromosome) were examined in the spleen DNA for evidence of heterozygosity. The heterozygous SNPs in the spleen were examined in the teratoma, in order to determine the last meiotic stage completed by the oocyte before initiating OT formation (Surti et al., 1990). Detailed information of SNP locations and sequence in the spleen and OT are provided in Supplementary Table 1.

Identification of *Tgkd* insertional site

This was accomplished by identifying the two *Tgkd*-genome junctional fragments on Southern blots of FVB-*Tgkd* DNA probed with fragments of the *Tgkd* transgene, constructing *Tgkd* subgenomic libraries in the λFixII vector (Stratagene, La Jolla, CA), and identifying clones containing the two junctional fragments.

Collection of embryos

Crosses were set up between hemizygous *Tgkd* and wildtype animals so that the parental origin of the *Tgkd* transgene was known. The day on which the plug was observed was noted as day 0.5. Embryonic day 13.5 (E13.5) embryos were collected 13 days after observation of the plug. E13.5 embryo heads were frozed at −80ºC until RNA extraction or protein extraction. Tail DNA was isolated from these embryos and used to determine presence or absence of *Tgkd*.

Collection of ovaries and oocytes

Whole ovary, germinal vesicle (GV)-stage oocytes and GCs were collected from immature females (21–23 day post partum) at designated time points following intra-peritoneal (IP) injection of 5IU pregnant mare serum gonadotropin (PMSG) (Calbiochem- 367222, LaJolla, CA) and 5IU of human chorionic gonadotropin (HCG) (Sigma- C5297, St Louis, MO) injection. GCs and oocytes were collected in M2 medium (Millipore-MR-015-D, Temecula, CA) following needle puncture of the ovaries. The oocytes were collected and the remaining GCs were pelleted and lysed in 1X Laemmli sample buffer.

Ovarian morphology was examined in hematoxylin and eosin (H&E)-stained paraffin sections of ovaries fixed overnight in 4% paraformaldehyde. Follicle counting and classification were performed on every fifth adjacent section of 5μm thickness according to an established system described by Pederson and Peters (Pedersen and Peters 1968).

Parthenogenetic activation of *Tgkd* oocytes was examined by isolating cumulus-oocyte-complexes (COC) from immature PD23 wildtype and *Tgkd* mice after 48 hours of PMSG stimulation. Oocytes were separated from surrounding cumulus cells after *in-vitro* maturation and the frequency of 2-cell embryos was determined after 24 hours of additional culture in KSOM (Embryomax- MR-106-D, Millipore) as described previously (Eppig et al., 1996).

ES cell derivation and generation of shRNA clones

129-*Tgkd*(mat) ES lines were derived from 129-*Tgkd* X 129 crosses and 129-*Tgkd*(pat) ES lines were derived from 129 X 129-*Tgkd* crosses. Homozygous *Tgkd* ES lines were derived from 129-*Tgkd* X 129-*Tgkd* crosses. ES cell lines were generated by collection of E3.5 blastocysts and ES cell lines were established using previously published methods (Nagy et al., 2003). Stable knockdown clones of INPP4B were obtained by the electroporation of linearized shRNA plasmid constructs TRCN0000080645 and TRCN0000080646 (Open Biosystems, Huntsville, AL) followed by isolation of puromycin-resistant colonies. Extent of knockdown of INPP4B was determined by immunoblot analysis.

IGF1 stimulation protocol

ES cells were passaged twice without feeders and then plated on 12 well plates coated with 0.1% gelatin. The cells were serum starved for 34 hours and then stimulated with 1μg/ul of mouse IGF1 (Sigma-I8779) for indicated periods.

Granulosa cell culture

This experiment was performed as described previously with minor modifications (Escamilla-Hernandez et al., 2008). This protocol enables selective enrichment of GCs by isolating and culturing GCs from wildtype and *Tgkd* ovaries and excludes oocytes, and the ovarian capsule from the analysis. Ovaries were harvested from immature females (day 21–23 postpartum) and incubated in 6mM EGTA and 0.5M Sucrose in DMEM/F12 (Cellgro-10-092-CV, Herndon, VA). The ovaries were punctured with needles to release GCs in DMEM/F12. The GCs were pelleted at 100g for 10 minutes and resuspended at a density 0.5 X 10^6 cells /well in DMEM/F12 +10%FBS. After overnight culture the cells were stimulated for indicated time points with DMEM/F12+ recombinant human FSH (LER-4161B) (50ng/μl-final concentration) (Kind gift from Dr. Anthony Zeleznik) and the cells were subsequently lysed in 1X Laemmli sample buffer.

For lentiviral infections, 10^6 GCs were centrifuged and then resuspended in DMEM/F12 containing 8 μg/ml polybrene (hexadimethrin bromide – Sigma H9268). The GCs were infected with lentivirus expressing shRNA constructs to *Inpp4b*, either TRCN0000080645

or TRCN0000080646 (Open Biosystems) at an MOI (multiplicity of infection) of 10 for 2 hours following which the lentivirus-cell suspension was plated in DMEM/F12 +10%FBS. After 48 hours of culture, the cells were stimulated with DMEM/F12+ FSH (50ng/μl) for the indicated times.

Bisulfite genomic sequencing

Bisulfite genomic sequencing was performed using the EpiTect Bisulfite Kits (Qiagen-59104, Valencia, CA) (Clark et al., 1994). Following bisulfite treatment, the RSV sequence was amplified with PCR primers flanking the RSV DMD (within the *Ig* and c-*myc* sequences). Primer sequences are provided in Supplementary Figure 6.

Real Time PCR

RNA was extracted using the RNeasy Micro kit (Qiagen). 1μg of RNA was converted to cDNA using the high capacity cDNA reverse transcription kit (Applied Biosystems, Foster City CA) in a reaction volume of 20μl. 2μl of the cDNA was used in a 10ul Real time PCR reaction. Real time PCR was performed using the SYBR Green master mix (Applied Biosystems) on the *7900HT* Fast Real-Time PCR System machine (Applied Biosystems). Steady-state transcript levels were measured by real-time PCR using oligonucleotide primers located across exons 23 and 24 of *Inpp4b* mRNA, a region common to all known forms of *Inpp4b* transcripts. The Alpha and Beta isoforms were assayed separately by amplification of their alternative terminal exons. The Pfaffl method was used to determine fold changes and the fold changes were determined as fold change over wildtype levels (Pfaffl 2001). TATA-binding protein (TBP) (E13.5 embryo studies) and beta glucuronidase (GUSB) (Ovary studies) were selected as housekeeping control genes. Primer sequences are provided in Supplementary Figure 6.

Immunoblot Analysis

E13.5 heads, ovaries and ES cell proteins were extracted using RIPA lysis buffer supplemented with complete protease inhibitor and Phosstop phosphatase inhibitor (Roche, Basel, Switzerland). Oocytes and GCs were lysed in 1X Laemmli sample buffer. Immunoblot analysis was performed as described previously (Cirio et al. 2008). Membranes were probed with the following antibodies: INPP4B (Brain and ES cells - Santa Cruz-sc12318, Santa cruz, CA), INPP4B (Ovary and GCs - Ferron and Vacher 2006), Phospho-AKT (Ser-473) (9271), phospho-FOXO1 (Ser-256) (9461), E2F1 (3742), Cyclin D2 (3741) (Cell Signaling technology, Beverly, MA) and Actin (Abcam, Cambridge, MA). The blots were stripped and reprobed with FOXO1 (2880), AKT (9272) (Cell Signaling technology) and $P27^{KIP}$ (Santa cruz-sc528). Anti–rabbit (GE healthcare: NA934V, Piscataway, NJ) or anti-goat (sc-2020) secondary antibodies were diluted in blocking solution (5% milk). Bound antibody was detected using the chemiluminescence detection kit ECL Plus (Amersham, Piscataway, NJ). Protein levels were determined by comparison of intensity on autoradiography films using the BioSpectrum 500 imager and VisionWorks®LS analysis software (UVP, LLC, Upland, CA).

BrdU Incorporation Assay

PD30 mice received an IP injection of 100mg/kg of BrdU (Sigma -B9285) and were killed 2 hours after injection. Ovaries were isolated and the BrdU incorporation was detected by immunohistochemistry

Immunohistochemistry

Ovaries were fixed in 4% PFA and embedded in paraffin. Immunohistochemistry was performed on 5μm sections using the Vectastain Elite ABC Kit (Vector laboratories,

Burlingame, CA) according to manufacturer instructions. Mouse anti-BrdU (Sigma- B2531) was used to evaluate cell proliferation and rabbit anti-cleaved caspase3 (Cell Signaling Technology- 9664) was used to determine the rate of apoptosis in follicles. Immunohistochemisty was performed on 4 non-adjacent sections and positive cells were counted in 25 follicles containing a clear oocyte. Rates of proliferation and apoptosis per follicle were determined by the number of positive cells in each preantral (Type 5) and antral follicle divided by the total number of cells in the follicle.

RNA *in situ* hybridization (ISH)

Ovaries from 7-week-old mice were dissected in M2 media, washed in 1X PBS and fixed in fresh 4% paraformaldehyde. PFA-fixed samples were immersed in 10%, then 20% sucrose in PBS, followed by OCT embedding. We used digoxigenin-labeled cRNA probes, synthesized using digoxigenin RNA labeling kit (Roche). Cryosections (10 μm) of the OCT-embedded placentas were used for ISH as previously described (Barak et al., 1999). Probes to *Inpp4b* isoforms α and β were designed complementary to their respective alternative terminal exons. Primer sequences used to amplify probe sequence from *Inpp4b* cDNA are provided in Supplementary Figure 6.

ELISA

P-AKT activation was measured in ES cell lysates using the PathScan® Phospho-Akt1 (Ser473) and Total Akt1 Sandwich ELISA Kit (Cell signaling: 7160 & 7170) according to manufacturer instructions.

Statistical analysis

Each experiment was repeated a minimum of 3 times. A mean and standard error was calculated. Significance was assessed using the Wilcoxon Rank-sum test. Results were considered significant (*) if the p value was less than 0.05.

Supplementary Material

Refer to Web version on PubMed Central for supplementary material.

Acknowledgments

The authors thank Dr. William Walker for help with immunoblotting experiments, Dr. Anthony Zeleznik for assistance with *in vitro* granulosa-cell experiments, and Dr. Katherine Himes and Mr. Erik Koppes for advice on *in situ* hybridization. We thank Dr. Jean Vacher (IRCM, Montreal Canada) for gift of the anti-INPP4B rabbit serum. This research was supported by a grant from the National Institutes of Health (USA) to JRC.

References

Barak Y, Nelson MC, Ong ES, Jones YZ, Ruiz-Lozano P, Chien KR, Koder A, Evans RM. PPAR gamma is required for placental, cardiac, and adipose tissue development. Mol Cell. 1999; 4(4): 585–595. [PubMed: 10549290]

Blake KI, Gerrard MP. Malignant germ cell tumors in two siblings. Med Pediatr Oncol. 1993; 21:299–300. [PubMed: 7682284]

Bourc'his D, Xu GL, Lin CS, Bollman B, Bestor TH. Dnmt3L and the establishment of maternal genomic imprints. Science. 2001; 294(5551):2536–2539. [PubMed: 11719692]

Brenner SH, Wallach RC. Familial benign cystic teratomata. J Gynaecol Obstet. 1983; 21:167–169.

Castrillon DH, Miao L, Kollipara R, Horner JW, DePinho RA. Suppression of ovarian follicle activation in mice by the transcription factor Foxo3a. Science. 2003; 301(5630):215–218. [PubMed: 12855809]

Carritt B, Parrington JM, Welch HM, Povey S. Diverse origins of multiple ovarian teratomas in a single individual. Proc Natl Acad Sci U S A. 1982; 79(23):7400–7404. [PubMed: 6961419]

Chaillet JR, Bader DS, Leder P. Regulation of genomic imprinting by gametic and embryonic processes. Genes Dev. 1995; 9(10):1177–1187. [PubMed: 7758943]

Cirio MC, Ratnam S, Ding F, Reinhart B, Navara C, Chaillet JR. Preimplantation expression of the somatic form of Dnmt1 suggests a role in the inheritance of genomic imprints. BMC Dev Biol. 2008; 8:9. [PubMed: 18221528]

Clark SJ, Harrison J, Paul CL, Frommer M. High sensitivity mapping of methylated cytosines. Nucleic Acids Res. 1994; 22:2990–2997. [PubMed: 8065911]

Colledge WH, Carlton MB, Udy GB, Evans MJ. Disruption of c-mos causes parthenogenetic development of unfertilized mouse eggs. Nature. 1994; 370:65–68. [PubMed: 8015609]

De Foy KA, Gayther SA, Colledge WH, Crockett S, Scott IV, Evans MJ, Ponder BA. Mutation analysis of the c-mos proto-oncogene in human ovarian teratomas. Br J Cancer. 1998; 77:1642–1644. [PubMed: 9635841]

Deka R, Chakravarti A, Surti U, Hauselman E, Reefer J, Majumder PP, Ferrell RE. Genetics and biology of human ovarian teratomas. II Molecular analysis of origin of nondisjunction and gene-centromere mapping of chromosome I markers. Am J Hum Genet. 1990; 47(4):644–655. [PubMed: 1977308]

Eppig JJ, Kozak LP, Eicher EM, Stevens LC. Ovarian teratomas in mice are derived from oocytes that have completed the first meiotic division. Nature. 1977; 269:517–518. [PubMed: 909601]

Eppig JJ, Wigglesworth K, Varnum DS, Nadeau JH. Genetic regulation of traits essential for spontaneous ovarian teratocarcinogenesis in strain LT/Sv mice: aberrant meiotic cell cycle, oocyte activation, and parthenogenetic development. Cancer Res. 1996; 56(21):5047–5054. [PubMed: 8895763]

Escamilla-Hernandez R, Little-Ihrig L, Orwig KE, Yue J, Chandran U, Zeleznik AJ. Constitutively active protein kinase A qualitatively mimics the effects of follicle-stimulating hormone on granulosa cell differentiation. Mol Endocrinol. 2008; 8:1842–1852. [PubMed: 18535249]

Fafalios MK, Olander EA, Melhem MF, Chaillet JR. Ovarian teratomas associated with the insertion of an imprinted transgene. Mamm Genome. 1996; 7:188–193. [PubMed: 8833238]

Fan HY, Liu Z, Cahill N, Richards JS. Targeted disruption of Pten in ovarian granulosa cells enhances ovulation and extends the life span of luteal cells. Mol Endocrinol. 2008a; 22:2128–2140. [PubMed: 18606860]

Fan HY, Shimada M, Liu Z, Cahill N, Noma N, Wu Y, Gossen J, Richards JS. Selective expression of KrasG12D in granulosa cells of the mouse ovary causes defects in follicle development and ovulation. Development. 2008b; 135(12):2127–37. [PubMed: 18506027]

Fedele CG, Ooms LM, Ho M, Vieusseux J, O'Toole SA, Millar EK, Lopez-Knowles E, Sriratana A, Gurung R, Baglietto L, Giles GG, Bailey CG, Rasko JE, Shields BJ, Price JT, Majerus PW, Sutherland RL, Tiganis T, McLean CA, Mitchell CA. Inositol polyphosphate 4-phosphatase II regulates PI3K/Akt signaling and is lost in human basal-like breast cancers. Proc Natl Acad Sci U S A. 2010; 107:22231–22236. [PubMed: 21127264]

Fehniger TA, Suzuki K, Ponnappan A, VanDeusen JB, Cooper MA, Florea SM, Freud AG, Robinson ML, Durbin J, Caligiuri MA. Fatal leukemia in interleukin 15 transgenic mice follows early expansions in natural killer and memory phenotype CD8+ T cells. J Exp Med. 2001; 193(2):219–231. [PubMed: 11208862]

Ferron M, Vacher J. Characterization of the murine Inpp4b gene and identification of a novel isoform. Gene. 2006; 376(1):152–161. [PubMed: 16631325]

Ferron M, Boudiffa M, Arsenault M, Rached M, Pata M, Giroux S, Elfassihi L, Kisseleva M, Majerus PW, Rousseau F, Vacher J. Inositol polyphosphate 4-phosphatase B as a regulator of bone mass in mice and humans. Cell Metab. 2011; 14(4):466–477. [PubMed: 21982707]

Gewinner C, Wang ZC, Richardson A, Teruya-Feldstein J, Etemadmoghadam D, Bowtell D, Barretina J, Lin WM, Rameh L, Salmena L, Pandolfi PP, Cantley LC. Evidence that inositol polyphosphate 4-phosphatase type II is a tumor suppressor that inhibits PI3K signaling. Cancer Cell. 2009; 16(2):115–125. [PubMed: 19647222]

Goldman DS, Kiessling AA, Millette CF, Cooper GM. Expression of c-mos RNA in germ cells of male and female mice. Proc Natl Acad Sci USA. 1987; 84:4509–4513. [PubMed: 2955407]

Gonzalez-Robayna IJ, Falender AE, Ochsner S, Firestone GL, Richards JS. Follicle- Stimulating hormone (FSH) stimulates phosphorylation and activation of protein kinase B (PKB/Akt) and serum and glucocorticoid-lnduced kinase (Sgk): evidence for A kinase-independent signaling by FSH in granulosa cells. Mol Endocrinol. 2000; 8:1283–1300. [PubMed: 10935551]

Hampl A, Eppig JJ. Analysis of the mechanism(s) of metaphase I arrest in maturing mouse oocytes. Development. 1996; 121:925–933. [PubMed: 7743936]

Han SJ, Vaccari S, Nedachi T, Andersen CB, Kovacina KS, Roth RA, Conti M. Protein kinase B/Akt phosphorylation of PDE3A and its role in mammalian oocyte maturation. EMBO J. 2006; 25(24): 5716–5725. [PubMed: 17124499]

Hashimoto N, Watanabe N, Furuta Y, Tamemoto H, Sagata N, Yokoyama M, Okazaki K, Nagayoshi M, Takeda N, Ikawa Y, Aizawai S. Parthenogenetic activation of oocytes in c-mos-deficient mice. Nature. 1994; 370:68–71. [PubMed: 8015610]

Heikinheimo M, Ermolaeva M, Bielinska M, Rahman NA, Narita N, Huhtaniemi IT, Tapanainen JS, Wilson DB. Expression and hormonal regulation of transcription factors GATA-4 and GATA-6 in the mouse ovary. Endocrinology. 1997; 138(8):3505–3514. [PubMed: 9231805]

Hodgson MC, Shao LJ, Frolov A, Li R, Peterson LE, Ayala G, Ittmann MM, Weigel NL, Agoulnik IU. Decreased Expression and Androgen Regulation of the Tumor Suppressor Gene INPP4B in Prostate Cancer. Cancer Res. 2011; 71:572–582. [PubMed: 21224358]

Hoffner L, Shen-Schwarz S, Deka R, Chakravarti A, Surti U. Genetics and biology of human ovarian teratomas. III Cytogenetics and origins of malignant ovarian germ cell tumors. Cancer Genet Cytogenet. 1992; 62(1):58–65. [PubMed: 1521236]

Hoshino Y, Yokoo M, Yoshida N, Sasada H, Matsumoto H, Sato E. Phosphatidylinositol 3-kinase and Akt participate in the FSH-induced meiotic maturation of mouse oocytes. Mol Reprod Dev. 2004; 69(1):77–86. [PubMed: 15278907]

Howlader, N.; Noone, AM.; Krapcho, M.; Neyman, N.; Aminou, R.; Waldron, W.; Altekruse, SF.; Kosary, CL.; Ruhl, J.; Tatalovich, Z.; Cho, H.; Mariotto, A.; Eisner, MP.; Lewis, DR.; Chen, HS.; Feuer, EJ.; Cronin, KA.; Edwards, BK. SEER Cancer Statistics Review, 1975–2008. National Cancer Institute; Bethesda MD: 2011.

Hsieh M, Lee D, Panigone S, Horner K, Chen R, Theologis A, Lee DC, Threadgill DW, Conti M. Luteinizing hormone-dependent activation of the epidermal growth factor network is essential for ovulation. Mol Cell Biol. 2007; 27(5):1914–1924. [PubMed: 17194751]

Hsu SY, Lai RJ, Finegold M, Hsueh AJ. Targeted overexpression of Bcl-2 in ovaries of transgenic mice leads to decreased follicle apoptosis, enhanced folliculogenesis, and increased germ cell tumorigenesis. Endocrinology. 1996; 137:4737–4843.

Huang H, Tindall DJ. Dynamic FoxO transcription factors. J Cell Sci. 2007; 120:2479–2487. [PubMed: 17646672]

Indinnimeo M, Cicchini C, Larcinese A, Kanakaki S, Ricci F, Mingazzini PL. Two twins with teratoma of the ovary. An unusual association: case report. Eur J Gynaecol Oncol. 2003; 24:199–201. [PubMed: 12701979]

John GB, Gallardo TD, Shirley LJ, Castrillon DH. Foxo3a is a PI3K-dependent molecular switch controlling the initiation of oocyte growth. Dev Biol. 2008; 321:197–204. [PubMed: 18601916]

Kalous J, Solc P, Baran V, Kubelka M, Schultz RM, Motlik J. PKB/AKT is involved in resumption of meiosis in mouse oocytes. Biol Cell. 2006; 98:111–123. [PubMed: 15842198]

Kennedy MK, Glaccum M, Brown SN, Butz EA, Viney JL, Embers M, Matsuki N, Charrier K, Sedger L, Willis CR, Brasel K, Morrissey PJ, Stocking K, Schuh JC, Joyce S, Peschon JJ. Reversible defects in natural killer and memory CD8 T cell lineages in interleukin 15-deficient mice. J Exp Med. 2000; 191:771–780. [PubMed: 10704459]

Lee GH, Bugni JM, Obata M, Nishimori H, Ogawa K, Drinkwater NR. Genetic dissection of susceptibility to murine ovarian teratomas that originate from parthenogenetic ocytes. Cancer Res. 1997; 57:590–593. [PubMed: 9044831]

Linder D, McCaw BK, Hecht F. Parthenogenetic origin of benign ovarian teratomas. N Engl J Med. 1975; 292:63–66. [PubMed: 162806]

Maehama T, Dixon JE. The tumor suppressor, PTEN/MMAC1, dephosphorylates the lipid second messenger, phosphatidylinositol 3,4,5-trisphosphate. J Biol Chem. 1998; 273(22):13375–13378. [PubMed: 9593664]

Manning BD, Cantley LC. AKT/PKB signaling: navigating downstream. Cell. 2007; 129(7):1261–1274. [PubMed: 17604717]

Muretto P, Chilosi M, Rabitti C, Tommasoni S, Colato C. Biovularity and “coalescence of primary follicles” in ovaries with mature teratomas. Int J Surg Pathol. 2001; 9(2):121–125. [PubMed: 11484499]

Nagy, A.; Gertsenstein, M.; Vinterstern, K.; Behringer, R. Manipulation of Mouse Embryos: A Laboratory Manual. Cold Spring Harbor, New York: Cold Spring Harbor Laboratory Press; 2003. p. 380-387.

Norris FA, Atkins RC, Majerus PW. The cDNA cloning and characterization of inositol polyphosphate 4-phosphatase type II. Evidence for conserved alternative splicing in the 4-phosphatase family. J Biol Chem. 1997; 272(38):23859–64. [PubMed: 9295334]

Ohteki T, Suzue K, Maki C, Ota T, Koyasu S. Critical role of IL-15-IL-15R for antigen-presenting cell functions in the innate immune response. Nat Immunol. 2001; 2(12):1138–1143. [PubMed: 11702064]

O’Neill GT, Kaufman MH. Ovulation and fertilization of primary and secondary oocytes in LT/Sv strain mice. Gamete Res. 1987; 18:27–36. [PubMed: 3507361]

Parrington JM, West LF, Povey S. The origin of ovarian teratomas. J Med Genet. 1984; 21(1):4–12. [PubMed: 6363699]

Pedersen T, Peters H. Proposal for a classification of oocytes and follicles in the mouse ovary. J Reprod Fertil. 1968; 17(3):555–557. [PubMed: 5715685]

Peltoketo H, Strauss L, Karjalainen R, Zhang M, Stamp GW, Segaloff DL, Poutanen M, Huhtaniemi IT. Female mice expressing constitutively active mutants of FSH receptor present with a phenotype of premature follicle depletion and estrogen excess. Endocrinology. 2010; 151:1872–1883. [PubMed: 20172968]

Pfaffl MW. A new mathematical model for relative quantification in real-time RT-PCR. Nucleic Acids Res. 2001; 29(9):e45. [PubMed: 11328886]

Plattner G, Oxorn H. Familial incidence of ovarian dermoid cysts. Can Med Assoc J. 1973; 108:892–893. [PubMed: 4707237]

Reddy P, Liu L, Adhikari D, Jagarlamudi K, Rajareddy S, Shen Y, Du C, Tang W, Hämäläinen T, Peng SL, Lan ZJ, Cooney AJ, Huhtaniemi I, Liu K. Oocyte-specific deletion of Pten causes premature activation of the primordial follicle pool. Science. 2008; 319:611–613. [PubMed: 18239123]

Richards JS, Sharma SC, Falender AE, Lo YH. Expression of FKHR, FKHRL1, and AFX genes in the rodent ovary: evidence for regulation by IGF-I, estrogen, and the gonadotropins. Mol Endocrinol. 2002; 16(3):580–599. [PubMed: 11875118]

Schmid-Braz AT, Cavalli LR, Cornélio DA, Wuicik L, Ribeiro EM, Bleggi-Torres LF, Lima RS, de Andrade Urban C, Haddad BR, Cavalli IJ. Comprehensive cytogenetic evaluation of mature ovarian tertaoma case. Cancer Genet Cytogen. 2002; 132:165–168.

Sherr CJ. D-type cyclins. Trends Biochem Sci. 1995; 20(5):187–190. [PubMed: 7610482]

Shimada M, Ito J, Yamashita Y, Okazaki T, Isobe N. Phosphatidylinositol 3-kinase in cumulus cells is responsible for both suppression of spontaneous maturation and induction of gonadotropin-stimulated maturation of porcine oocytes. J Endocrinol. 2003; 179(1):25–34. [PubMed: 14529562]

Simon A, Ohel G, Neri A, Schenker JG. Familial occurrence of mature ovarian teratoma. Obstet Gynecol. 1985; 66:278–279. [PubMed: 4022488]

Stettner AR, Hartenbach EM, Schink JC, Huddart R, Becker J, Pauli R, Long R, Laxova R. Familial ovarian germ cell cancer: report and review. Am J Med Genet. 1999; 84:43–46. [PubMed: 10213045]

Stevens LC, Varnum DS. The development of teratomas from parthenogenetically activated ovarian mouse eggs. Dev Biol. 1974; 37:369–380. [PubMed: 4826282]

Surti U, Hoffner L, Chakravarti A, Ferrell RE. Genetics and biology of human ovarian teratomas. I Cytogenetic analysis and mechanism of origin. Am J Hum Genet. 1990; 47(4):635–643. [PubMed: 2220805]

Thurisch B, Liang SY, Sarioglu N, Schomburg L, Bungert J, Dame C. Transgenic mice expressing small interfering RNA against Gata4 point to a crucial role of Gata4 in the heart and gonads. J Mol Endocrinol. 2009; 43:157–169. [PubMed: 19491195]

Ulbright TM. Germ cell tumors of the gonads: a selective review emphasizing problems in differential diagnosis, newly appreciated, and controversial issues. Mod Pathol. 2005; 18 (Suppl 2):S61–S79. [PubMed: 15761467]

Youngson NA, Vickaryous N, van der Horst A, Epp T, Harten S, Fleming JS, Khanna KK, de Kretser DM, Whitelaw E. A missense mutation in the transcription factor Foxo3a causes teratomas and oocyte abnormalities in mice. Mamm Genome. 2011; 22(3–4):235–248. [PubMed: 21347845]

Zeleznik AJ, Saxena D, Little-Ihrig L. Protein kinase B is obligatory for follicle stimulating hormone-induced granulosa cell differentiation. Endocrinology. 2003; 144(9):3985–3994. [PubMed: 12933673]

HIGHLIGHTS

- A random *Tgkd* transgene insertion lowers inositol phosphatase *Inpp4b* levels
- Decreased *Inpp4b* in granulosa cells linked to hyperactive PI3-kinase/AKT signaling
- Granulosa cell proliferation/apoptosis ratio increases in FVB-*Tgkd* ovaries
- Follicular defects such as trapped oocytes in corpus lutea seen in FVB-*Tgkd* ovaries
- Teratomas develop from meiotically mature oocytes in *Tgkd* follicles
- Trapped oocyte phenotype & high oocyte parthenogenesis may cause ovarian teratomas

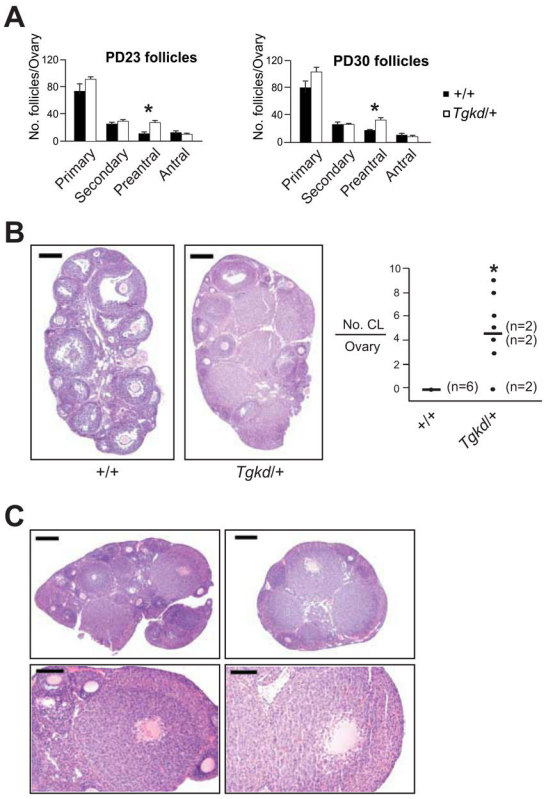

Figure 1.

Premature corpora lutea formation and luteinized unruptured follicles were observed in OT susceptible *Tgkd* mice. **(A)** Classification and numbers of ovarian follicles in the OT susceptible *Tgkd* strain compared to wildtype mice (n>6 ovaries). (**B)** Corpora lutea formation was observed in the *Tgkd* strain (n=10 ovaries) at postnatal day 30 (PD30) but not in wildtype wildtype PD30 mice (n=6) (Scale bar: 200μm). **(C)** The ovaries of *Tgkd* mice exhibited unruptured lutenized follicles, which contained oocytes trapped inside the corpora lutea (scale bar in upper panels 200μm; scale bar in lower panels 100μm). * - $p<0.05$.

A

Tgkd ovarian teratoma	Genotype[(b/a)] Pericentric	Distal
1	0/11	6/7
2	0/11	7/7
3	1/12	6/6
4	2/11	4/4
5	0/7	5/5
6	1/7	6/8
7	0/8	6/8

[a] Number of heterozygous SNPs in spleen of mouse with ovarian teratoma (OT)

[b] Number of SNPs heterozygous in both OT and spleen of host *Tgkd* female mouse

B

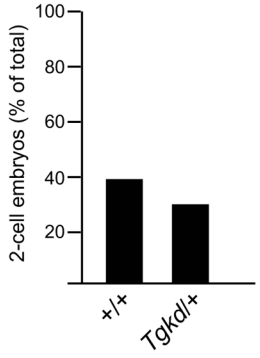

Figure 2.

OTs arise from mature oocytes that have completed meiosis 1. **(A)** Heterozygous pericentric and distal SNPs were identified in the spleens of 7 females with OTs from the cross between F1 (FVB-*Tgkd* X C57BL/6) and FVB mice. Genotypes (heterozygous or homozygous FVB) of these SNPs was then determined in each of the paired OTs. **(B)** Parthenogenetic activation and development to 2-cell stage was examined in wildtype (43 cumulus-oocyte complexes from 4 females) and *Tgkd* oocytes (37 cumulus-oocyte complexes from 4 females).

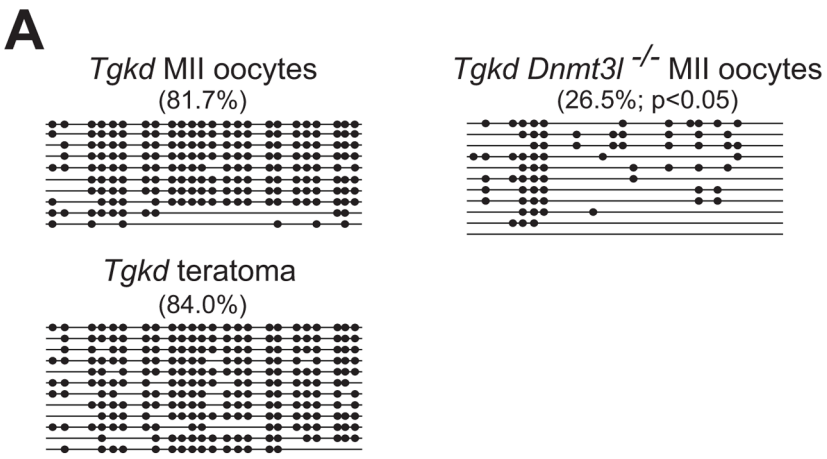

B

Genotype	OT incidence (%)
Tgkd, *Dnmt3l* $^{+/+}$	12/80 (15)
Tgkd, *Dnmt3l* $^{+/-}$	5/31 (16)
Tgkd, *Dnmt3l* $^{-/-}$	0/14 (0)

Figure 3.

Role of *Tgkd* transgene methylation in OT formation in the *Tgkd* strain. **(A)** Methylation of RSV region of *Tgkd* in MII oocytes (from 4 *Tgkd* mice), teratomas (from 2 *Tgkd* mice) and MII oocytes (from 2 *Tgkd*, *Dnmt3l*$^{-/-}$ mice). **(B)** The OT phenotype is present in 15% of *Tgkd* hemizygous females but is lost in the *Dnmt3l* $^{-/-}$ background. *- p value < 0.05.

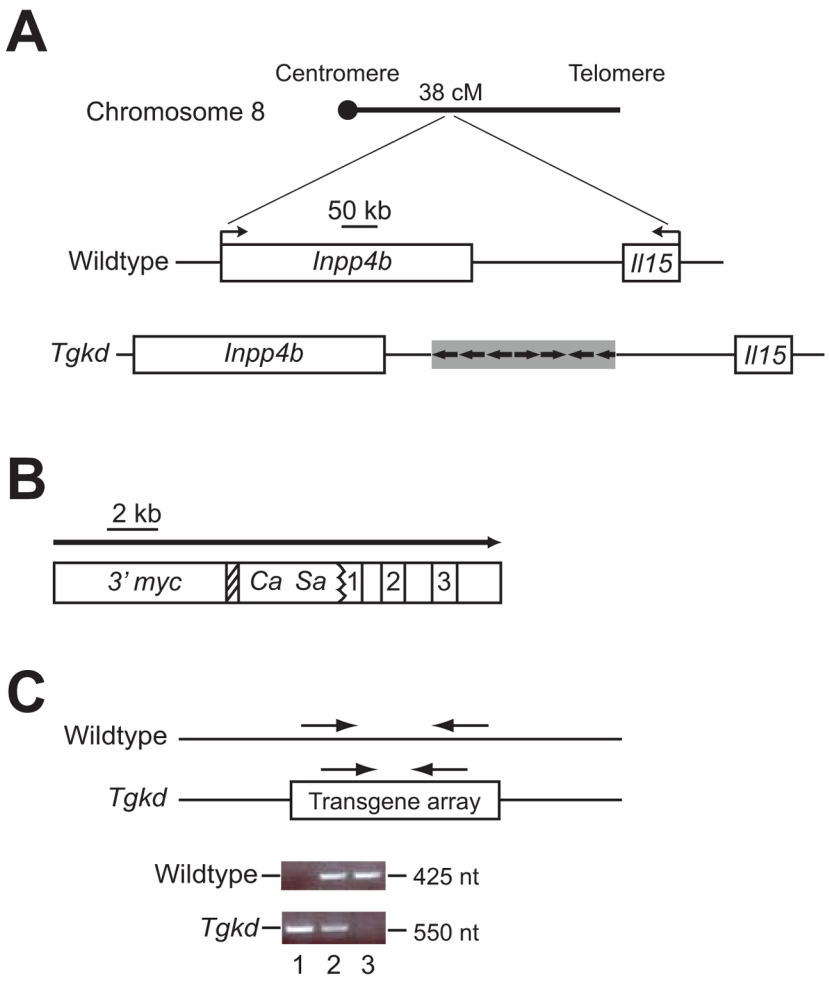

Figure 4.

Schematics of *Tgkd* transgene insertion site on chromosome 8. **(A)** The *Tgkd* allele is inserted on chromosome 8 as a transgene tandem array in head- head, tail-tail or head-tail orientation. Each arrow represents a single copy of the transgene. **(B)** Structure of the modified RSV *Igmyc* transgene used to generate the *Tgkd* line. **(C)** PCR analysis was used for genotyping the *Tgkd* transgene in the *Tgkd* strain. Lane 1 represents a mouse sample without the transgene, lane 2 represents a hemizygous *Tgkd* DNA sample and lane 3 represents a homozygous *Tgkd* DNA sample.

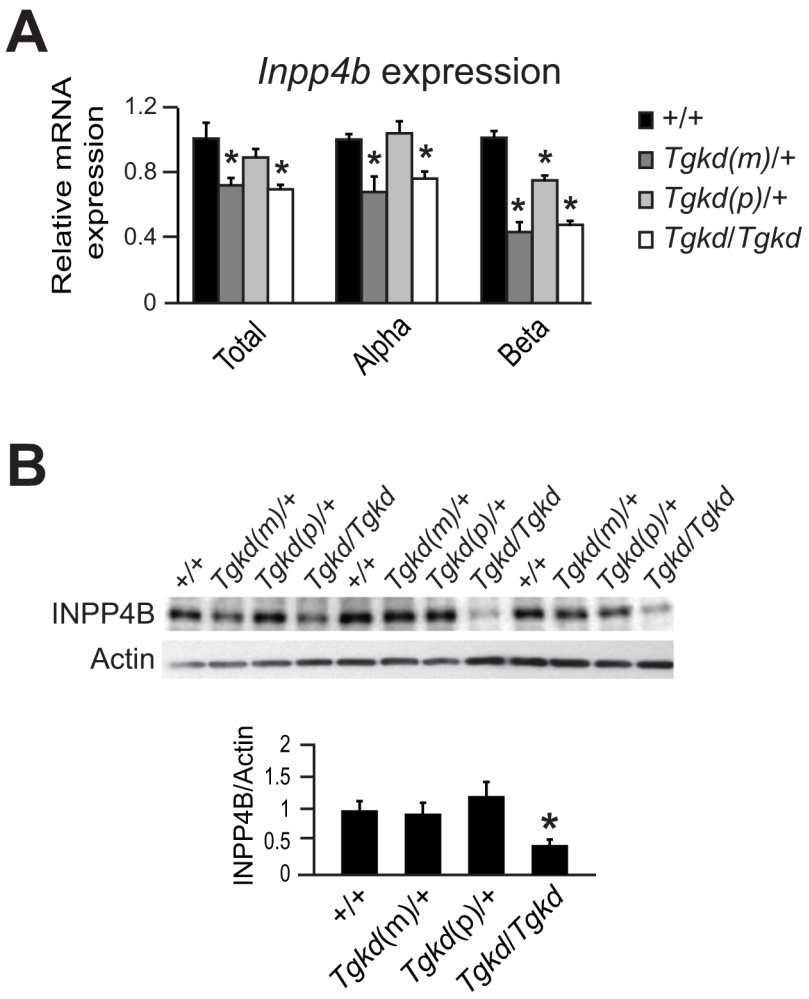

Figure 5.

Expression of *Inpp4b* in *Tgkd* embryos. **(A)** *Inpp4b* total transcript and levels of α and β isoforms were measured in homozygous and hemizygous *Tgkd* E13.5 embryo heads (+/+-wildtype; *Tgkd*(m)/+-maternally inherited *Tgkd; Tgkd*(p)/+-paternally inherited *Tgkd*; and *Tgkd*/*Tgkd* -homozygous *Tgkd*) (n>3 mice/genotype). **(B)** INPP4B protein levels in homozygous and hemizygous *Tgkd* E13.5 embryo heads (n=3). * - p value <0.05

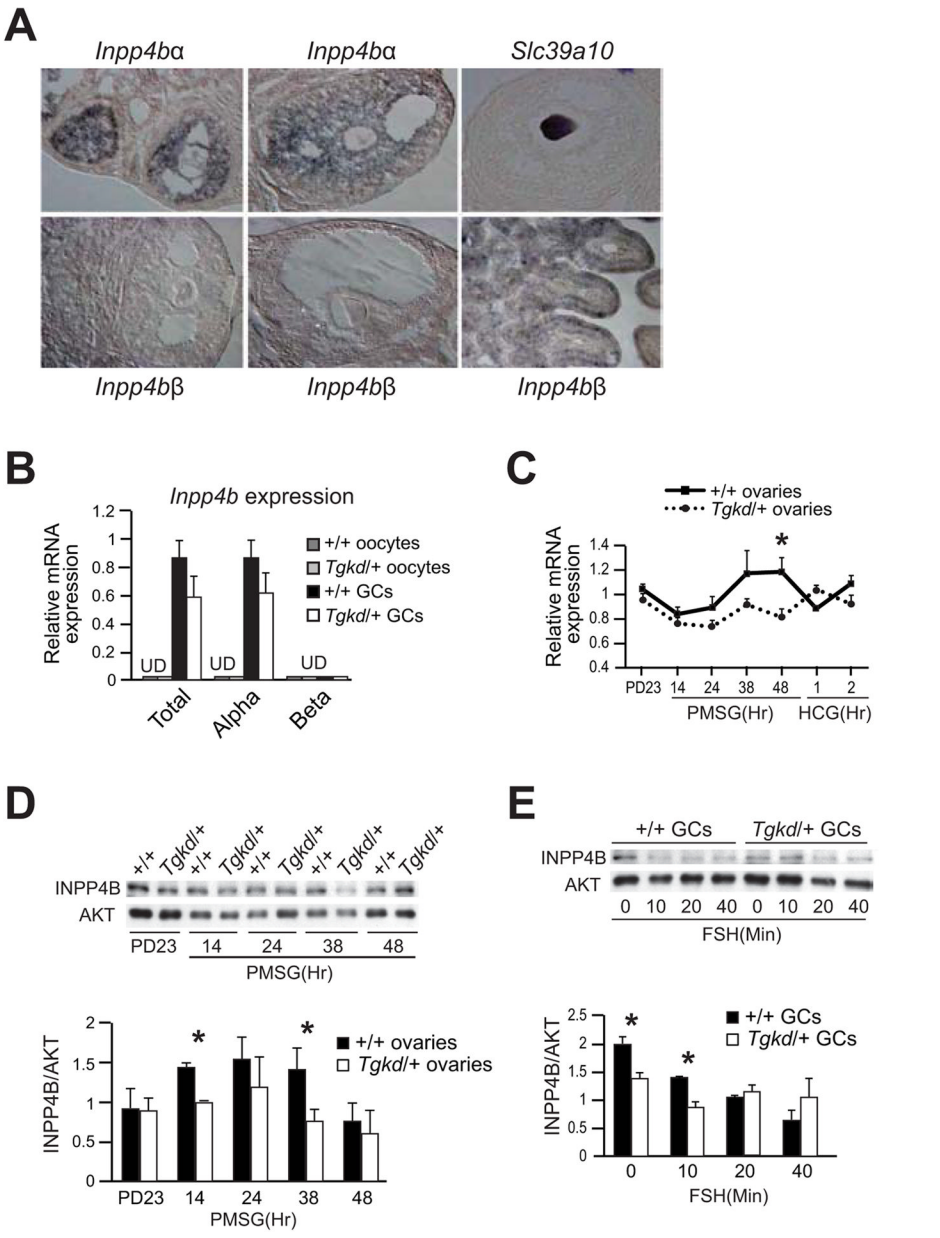

Figure 6.

Inpp4b expression in the wildtype and *Tgkd* ovaries. **(A)** *Inpp4b* α and β isoform expression in the ovarian follicle measured by *in situ* hybridization in 7-week old wildtype ovaries. Top right panel: Oocyte specific probe: *Slc39a10* to depict oocyte specific staining. Lower right panel: Small Intestine as positive control for *Inpp4bβ* probe **(B**) Real-time PCR quantitation of *Inpp4b* in GCs and oocytes in PD30 wildtype and *Tgkd* ovaries. **(C)** Real-time PCR quantitation of *Inpp4b* (*Inpp4b*α) in wildtype and *Tgkd* ovaries during the course of PMSG stimulation (n>3 mice/time point). **(D)** INPP4B protein levels in wildtype and *Tgkd* ovaries during PMSG stimulation (n=3). **(E)** Measurement of INPP4B protein on enriching the GCs in culture (n=3). * - p value <0.05.

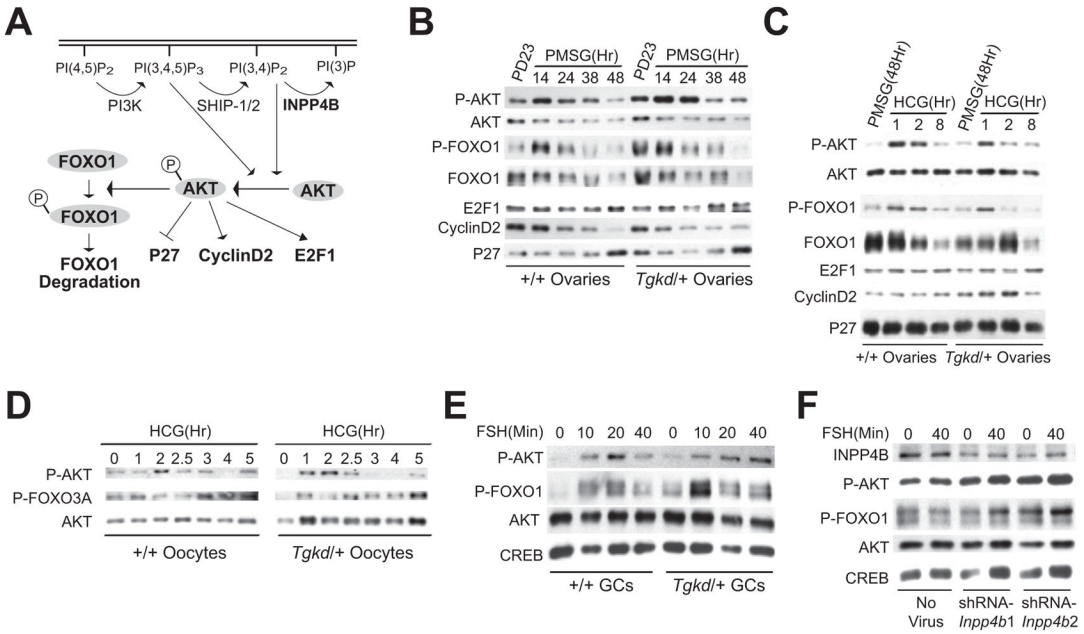

Figure 7.

Activation of the PI3K/AKT pathway in *Tgkd* ovaries. (**A)** Pathway depicting regulation of INPP4B on Phospho-AKT activation and its downstream targets. **(B)** Dynamics of the PI3K/AKT pathway was measured in wildtype and *Tgkd* ovaries in immature mice and on PMSG stimulation by investigating the levels of P-AKT, P-FOXO1, FOXO1, E2F1, Cyclin D2 and P27 (n=3 mice/time point; ovaries from single female per lane). **(C)** After 48 hours of PMSG stimulation; the mice were injected with HCG and the activation of the PI3K/AKT pathway was surveyed (n=3). **(D)** The dynamics of P-AKT phosphorylation was examined in wildtype and *Tgkd* oocytes (20 oocytes/lane). **(E)** P-AKT and P-FOXO1 activation were measured after FSH stimulation in cultured GCs from wildtype and *Tgkd* mice (n=3). **(F)** Lentiviral mediated shRNA downregulation of *Inpp4b* in wildtype GCs led to the activation of the PI3-kinase pathway similar to the levels seen in *Tgkd* GCs (n=3).

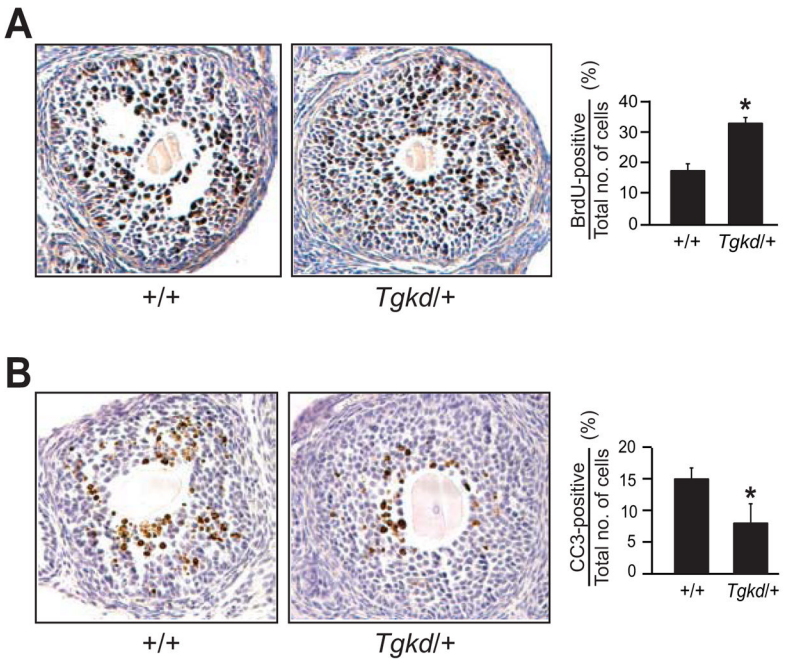

Figure 8.

Hyperactivation of the PI3K/AKT pathway in *Tgkd* ovaries leads to an increase in proliferation and decrease in apoptosis in *Tgkd* GCs. **(A)** Quantification of rate of granulosa cell proliferation in PD30 wildtype and *Tgkd* follicles measured by bromodeoxyuridine (Brdu) staining (n=25 follicles). **(B)** Quantification of rate of granulosa cell apoptosis in wildtype and *Tgkd* follicles measured by Cleaved Caspase 3 (CC3) staining (n=25 follicles). * - p value <0.05.